The Damage Zone in Microlayer Composites of Polycarbonate and Styrene–Acrylonitrile

E. SHIN,* A. HILTNER,** and E. BAER

Department of Macromolecular Science and Center for Applied Polymer Research, Case Western Reserve University, Cleveland, Ohio 44106

SYNOPSIS

The irreversible deformation behavior of coextruded microlayer composites, consisting of 49 alternating layers of polycarbonate (PC) and styrene–acrylonitrile polymer (SAN), was examined in the triaxial stress state achieved at a semicircular notch during slow tensile loading. Variations in the proportions of PC and SAN were manifest as changes in the relative thicknesses of PC and SAN layers. When the SAN layers were thicker than the PC layers (PC/SAN 25/75 v/v) or the layer thicknesses were about the same (53/47 v/v) the composites were only slightly more ductile than SAN and the deformation behavior of the layers mimicked that of the components. Examination of optical micrographs showed that the damage zone closely resembled that of SAN and consisted of internal notch crazes in the SAN layers that grew out from the notch surface in conformity with a mean stress condition. Shear processes became more evident when the PC layers were thicker than the SAN layers (PC/SAN 65/35 and 74/26 v/v). An unusual transition was observed in the SAN layers from internal notch crazing to interactive crazing and shear banding. The internal notch crazes ceased to grow when they terminated in a pair of microshear bands in the SAN layer. Subsequently a macroscopic shear-yielding mode was observed as two sets of intersecting slip lines that grew out from the notch surface in both PC and SAN layers. Stress intensification caused by the plastic zone was responsible for the appearance of a second family of internal crazes in the SAN layers that originated in front of the notch tip.

INTRODUCTION

Microlayer coextrusion is an advanced coextrusion process that differs from the conventional multilayer coextrusion in that many more layers, usually more than 50 but sometimes as many as several thousand, are produced in a single extrusion step. Recently, a study of thick microlayer sheet was undertaken in which polycarbonate (PC), a tough polymer, was combined with styrene–acrylonitrile copolymer (SAN), a brittle material that exhibits excellent interfacial adhesion to polycarbonate.[1-5] Not surprisingly, the tensile and impact properties showed a brittle-to-ductile transition when the PC/SAN volume ratio was increased.[2] In a subsequent study, the layer thickness was changed by varying the total number of layers while the overall composition was maintained constant.[3] In this case, the microlayer composite became increasingly ductile as the layers were made thinner due to a change in the deformation mechanism of the SAN layers from crazing to cooperative shearing. One manifestation of the synergistic effects with thinner layers was improved fracture toughness.[4] Energy absorbing mechanisms associated with the damage zone ahead of the fatigue crack played an important role in the resistance to crack propagation. Specifically, extensive plastic deformation of both SAN and PC layers ahead of the crack, together with ductile fracture of both components, enhanced the fracture toughness.

In order to characterize prefracture deformation processes and the resulting damage zone in a triaxial

* Present address: Composites Program, Michigan Molecular Institute, Midland, MI 48640-2696.

** To whom correspondence should be addressed.

Journal of Applied Polymer Science, Vol. 47, 245–267 (1993)
 CCC 0021-8995/93/020245-23

stress state while minimizing the tendency for crack growth, it is convenient to examine the damage zone that forms in the circular or semicircular notch geometry. This geometry has been used to clarify the shear-yielding modes in polycarbonate, including the effects of thickness, in terms of plasticity concepts.[6] The same geometry was used to examine crazing in styrene–acrylonitrile copolymer under a triaxial stress state.[7] In this case a different analytic approach was required. The plane-strain, elastic-stress distribution revealed that the stress state at the craze tips satisfied a constant mean stress condition; the critical mean stress for craze tip growth was determined to be about 35 MPa.

The approach that has been successfully used to examine irreversible deformation of the microlayer component polymers in a triaxial stress state was extended in the present study to the microlayer composites of PC and SAN. Composites with 49 alternating layers of the two components in varying volume ratios were used to characterize the damage zone as the composition was gradually changed from predominantly the crazing SAN component to predominantly the ductile PC component.

EXPERIMENTAL

Microlayer composites were supplied by The Dow Chemical Company in the form of coextruded sheets. The sheets were approximately 1.20 mm thick with alternating layers of PC and SAN; the outermost layer was PC in all cases. The PC was Merlon™ (Mobay Chemical Company, Pittsburgh, PA) M-40 and the SAN was Tyril™ (Dow Chemical Company, Midland, MI) 867-B. The SAN composition, 25% acrylonitrile by weight, was chosen for maximum adhesion to PC.[8] Nominal compositions taken from the feed rates to the extruders were provided by Dow, Table I. Compositions on a volume basis were determined directly from micrographs by measuring the thickness of individual layers in cross sections through the thickness. Since the thickness of individual SAN and PC layers varied somewhat from the edge to the center of the sheet, average values of the composition and layer thickness are reported in Table I. These values were used when required in calculations. Sheets of PC and SAN alone were prepared by the same coextrusion process and served as the controls. Although prepared by the same process, the controls did not display the layered structure of the composites.

Tensile tests of notched rectangular specimens, 100 mm × 20 mm were carried out on an Instron Testing Machine. A single 1 mm radius, semicircular notch was machined midway along one edge using a high-speed, steel end mill. The damage zone at the notch was photographed during deformation with a traveling optical microscope in the transmission mode. Typically, photographs were obtained both with the focus on the surface and adjusted to the center of the thickness. A final magnification of 130× was achieved in the photographic prints used for analysis. The optical micrographs were analyzed for the positions of the craze tips and for the craze trajectories as described previously.[7]

In some cases, specimens were loaded to specific positions on the stress-displacement curve and removed from the Instron for further characterization of the damage zone. A small section containing the damage zone was trimmed with a fine jewelry saw, the section was then microtomed in the yz plane at

Table I Microlayer Compositions and Mechanical Data

Composition PC/SAN v % (Layer Thickness μm)		Young's Modulus,	
As Given	As Measured	E (GPa)	Poisson's Ratio, ν
27/73	25/75 (11/34)	3.11[a]	0.363[a]
40/60	53/47 (23/22)	2.86[a]	0.377[a]
54/46	65/35 (27/15)	2.75[a]	0.383[a]
65/35	74/26 (33/13)	2.67[a]	0.387[a]
	SAN	3.34	0.35
	PC	2.43	0.40

[a] Calculated by the Rule of Mixtures:

$E = v_{SAN}E_{SAN} + v_{PC}E_{PC}$, and $\nu = v_{SAN}\nu_{SAN} + v_{PC}\nu_{PC}$.

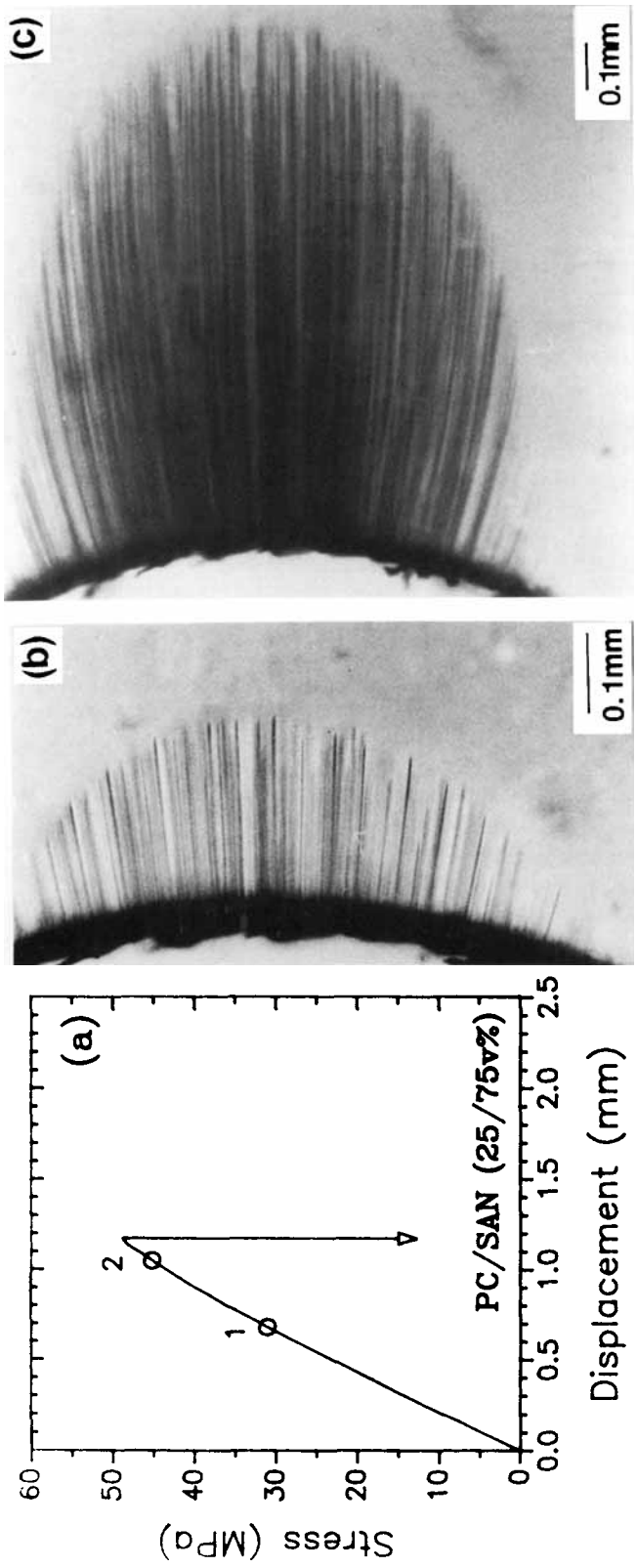

Figure 1 Tensile deformation of PC/SAN 25/75 with a semicircular notch. (a) The remote stress vs. displacement curve; (b) optical micrograph of the notch tip at position 1, 31.0 MPa; and (c) optical micrograph of the notch tip at position 2, 45.2 MPa.

the desired distance from the notch root. An RMC ultramicrotome (MT6000-XL) was used for this purpose.

RESULTS

PC/SAN 25/75 Composition

A typical stress-displacement curve of notched PC/SAN 25/75 in uniform tension [Fig. 1(a)] was initially linear with a slight nonlinear region prior to the brittle fracture. The stress and displacement at fracture were somewhat higher than for SAN (Table II), an effect that was also observed in unnotched tensile tests.[2] The points on the stress-displacement curve indicate the positions at which the damage zone at the notch was photographed during deformation.

The first damage was observed at a remote stress of about 23 MPa and consisted of a family of continuous lines that emanated from the notch surface [Fig. 1(b)]. These were similar to the internal notch crazes in SAN[7] but were much denser in the microlayer composite. Furthermore, the crazes did not follow straight lines, as they had in SAN, but were slightly curved even when quite short. The damage zone defined by the tips of the internal crazes was initially crescent shaped, but as the remote stress increased the damage zone gradually took on a somewhat ovoid shape [Fig. 1(c)].

A cross section of the damage zone in a specimen that had been loaded to 36 MPa is shown in Figure 2. The section, which was made about 30 μm from the notch tip, shows that the crazes extended through the thickness of individual SAN layers but were not in registry from one SAN layer to the next.

Table II Stress and Displacement at Fracture of Notched 49-Layer PC/SAN Composites

Composition (PC/SAN v %)	Stress at Fracture (MPa)		Displacement at Fracture (mm)
	Average	Local (SAN)[a]	
SAN[b]	41.7	41.7	0.84
25/75	48.8	52.4	1.17
53/47	51.4	60.0	1.37
65/35	48.2	58.5	1.36
74/26	57.9	72.4	1.98

[a] Values calculated for SAN layer using the Rule of Mixtures.
[b] Shin, Hiltner, and Baer.[7]

The two or three SAN layers closest to the edge contained noticeably fewer crazes; otherwise, the density of crazes in the SAN layer and the y-dimension of the crazed zone did not vary significantly through the thickness. There was no evidence of delamination where the craze tip impinged on the SAN–PC interface, instead a pair of microshear bands frequently initiated at this point and grew into the PC layer.

Profiles of the internal notch crazes of a typical damage zone were constructed by locating each craze in successive cross sections, as described previously.[7] The point of craze initiation on the notch surface was identified by the perpendicular distance from the x-axis given by h (mm) = sin θ [insert, Fig. 3(a)]. Crazes with growth planes close to the x-axis ($\theta \sim 0$), shown in Figure 3(a), included the longest crazes, although there were also a few shorter crazes. Crazes located midway between the x-axis and the boundary of the damage zone ($\theta \sim 6°$), and crazes near the boundary of the zone where the crazes were shortest ($\theta > 12°$) are shown in Figures 3(b) and 3(c), respectively. Although the craze length depended on the angle θ of the craze plane, it was characteristic that for any particular angle the maximum craze length did not vary through the thickness of the multilayer composite sheet. This suggested that except for the few layers closest to the surface, the SAN layers were in a triaxial stress state that did not vary through the thickness. Although it is unusual to associate the plane-strain state with thin layers, in this situation constraint in the thickness direction was provided by good adhesion between the alternating SAN and PC layers.

At higher stresses close to fracture, about 40 MPa, the craze lines thickened and darkened somewhat suggesting that some microdelamination at the SAN–PC interface might have occurred. Subsequently at about 47 MPa macrodelamination occurred at the notch tip, followed at about 49 MPa by brittle fracture that was characterized by very rapid crack propagation but no bifurcation of the crack path as had been typical of SAN.[7]

PC/SAN 53/47 Composition

The stress-displacement curve of this composition [Fig. 4(a)] was similar to that of the PC/SAN 25/75 microlayer except that as the proportion of PC increased, the initial slope gradually decreased and the stress and displacement at fracture gradually increased. The initial damage observed was again a family of internal notch crazes that emanated from the notch surface at a remote stress of about 23 MPa

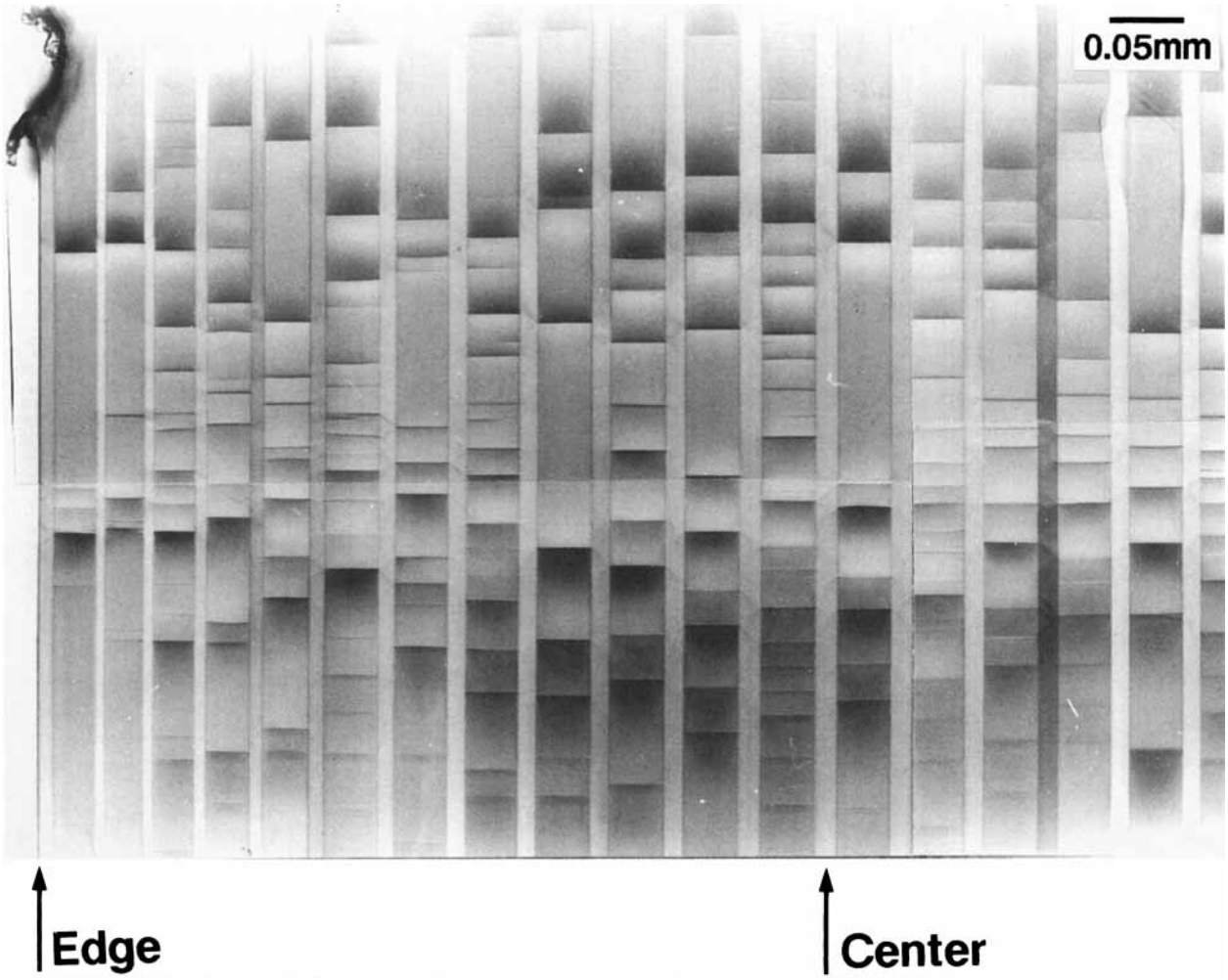

Figure 2 Microtomed cross section through the damage zone of PC/SAN 25/75 about 30 μm from the notch tip. The damage zone was created by loading the specimen to 36.0 MPa.

and grew away from the notch as the stress increased. The initial crescent shape of the zone defined by the craze tips [Fig. 4(b)] and the ovoid shape at higher stresses [Fig. 4(c)] were indistinguishable from the zone that formed in the PC/SAN 25/75 composite.

Failure at higher stresses occurred in a manner that was similar to the 25/75 composition with microdelamination at the crazes at about 41 MPa, macrodelamination at the notch tip at about 48 MPa, and brittle fracture at 50 MPa.

PC/SAN 65/35 Composition

The stress-displacement curve was similar to those of the other compositions [Fig. 5(a)] and a family of internal notch crazes was again the first damage observed in the PC/SAN 65/35 composite at a remote stress of about 23 MPa. The initial crescent shape of the zone defined by the craze tips was the same as in other compositions [Fig. 5(b)], although the craze density was noticeably lower and there appeared to be more variation in craze length with more crazes of shorter length. As the zone grew away from the notch, the crazes near the edge of the zone were longer than in the other compositions, and closer in length to crazes that grew close to the x-axis. This gave the zone a blunter shape [Fig. 5(c)]. Curvature was very evident in the crazes near the edge of the zone: their length emphasized the manner in which they curved over and grew almost parallel to the x-axis.

While most of the crazes grew away from the notch as the stress increased, a few of the crazes

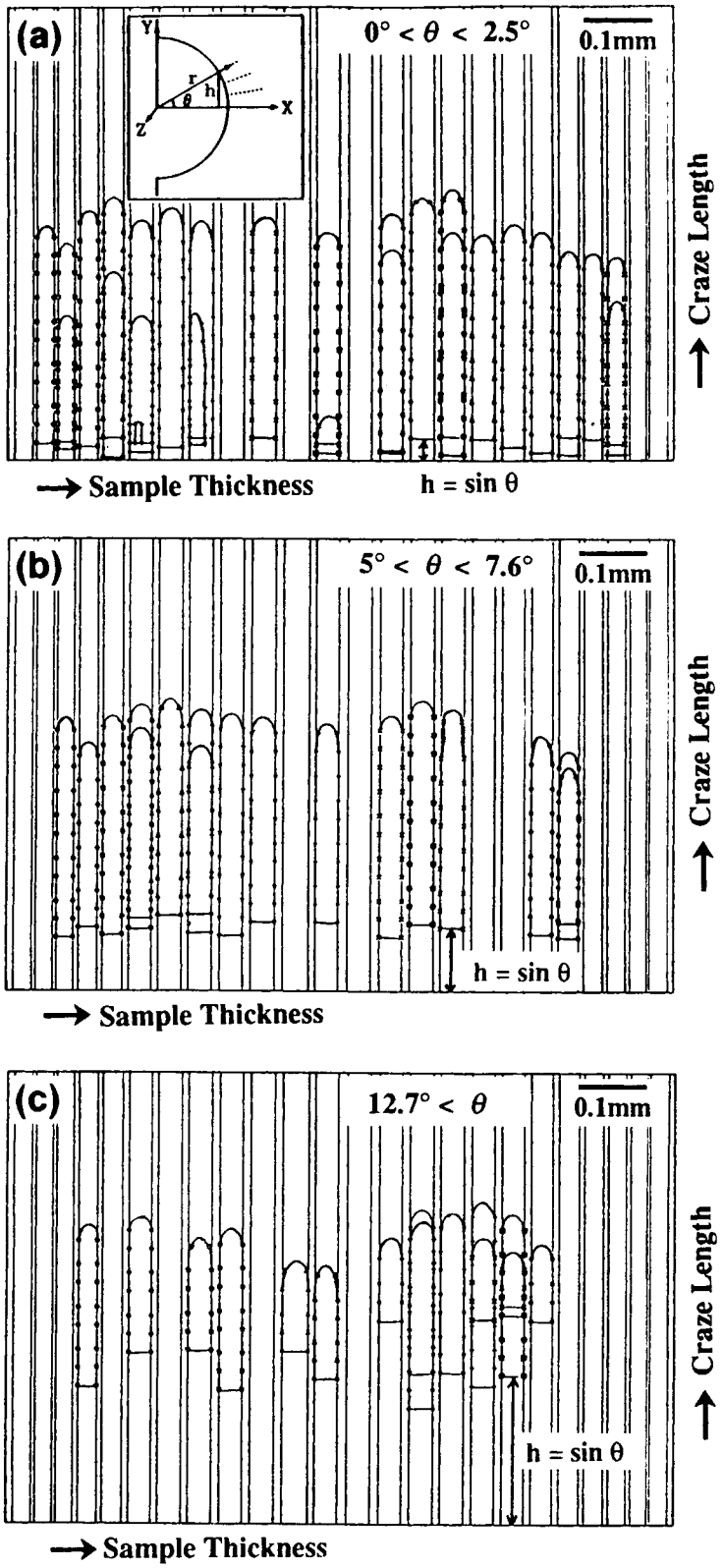

Figure 3 Profiles of internal notch crazes in PC/SAN 25/75 loaded to 36.0 MPa. (a) Crazes in the center of the damage zone close to the x-axis; (b) crazes located between the x-axis and the edge of the damage zone; and (c) crazes near the edge of the damage zone.

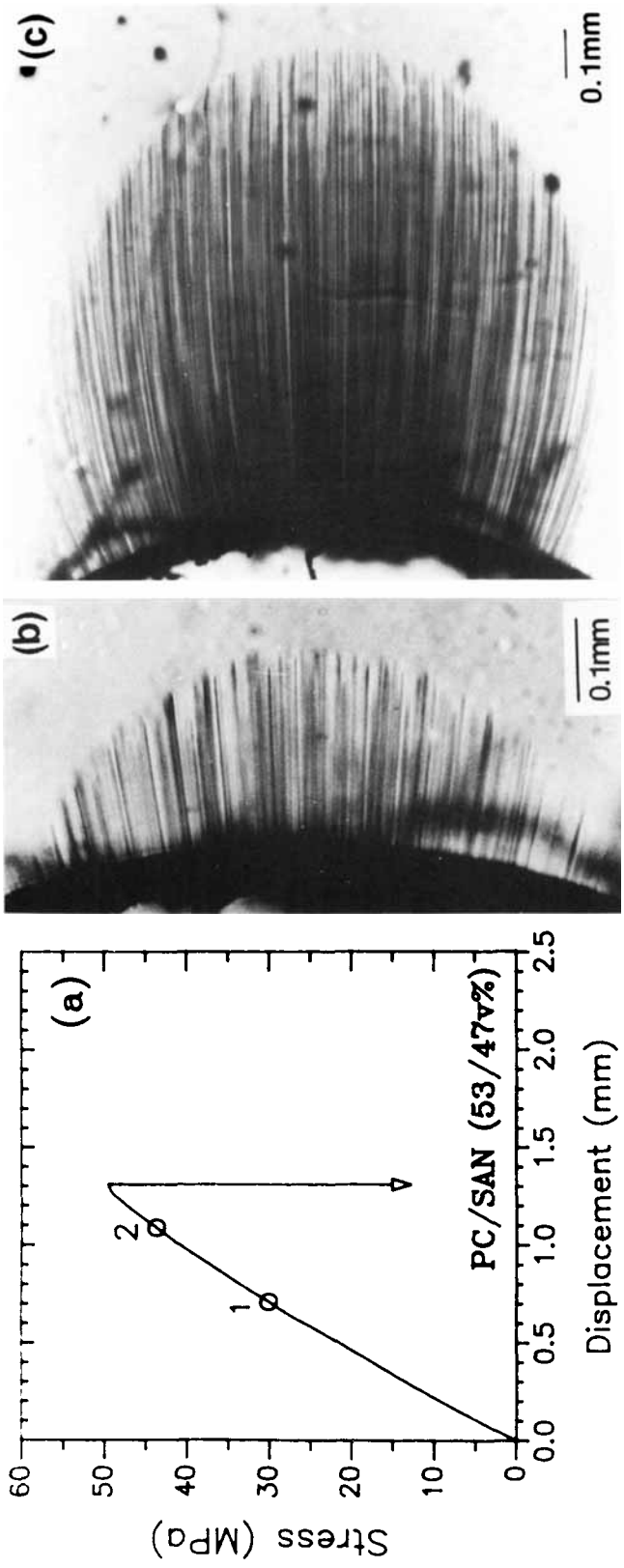

Figure 4 Tensile deformation of PC/SAN 53/47 with a semicircular notch. (a) The remote stress vs. displacement curve; (b) optical micrograph of the notch tip at position 1, 30.0 MPa; and (c) optical micrograph of the notch tip at position 2, 43.6 MPa.

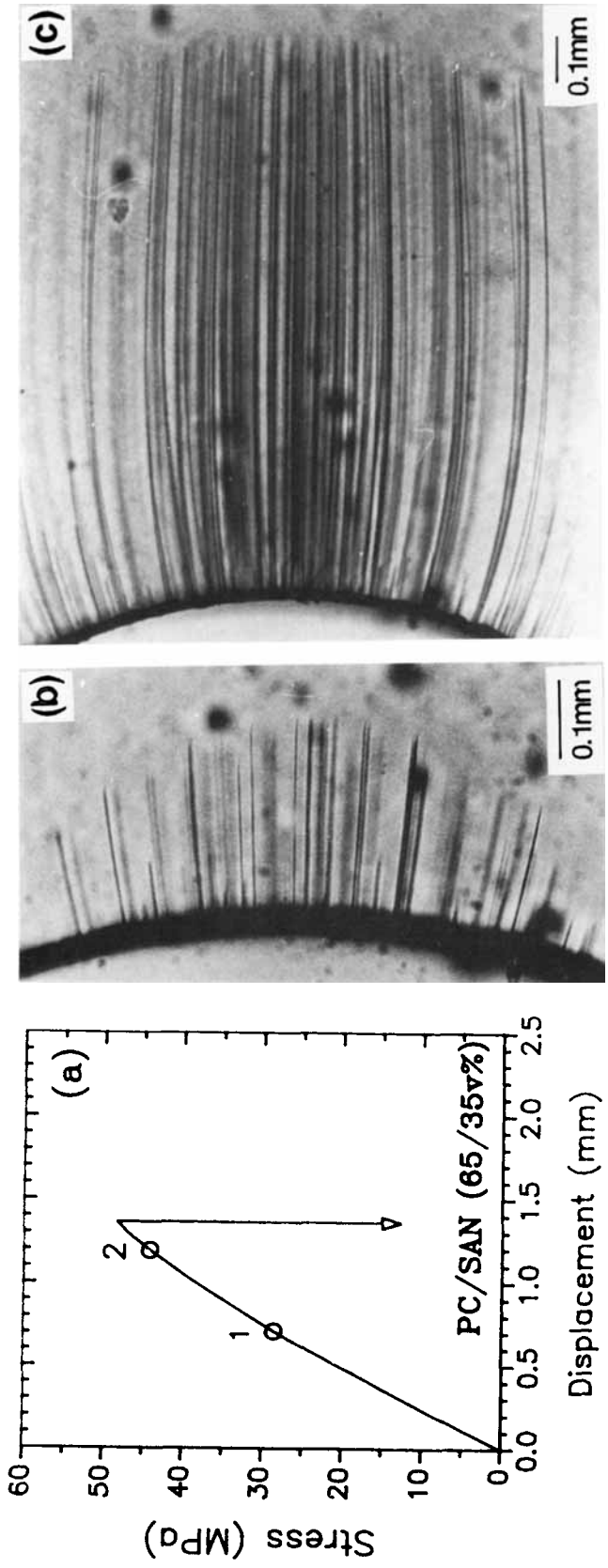

Figure 5 Tensile deformation of PC/SAN 65/35 with a semicircular notch. (a) The remote stress vs. displacement curve; (b) optical micrograph of the notch tip at position 1, 28.5 MPa; and (c) optical micrograph of the notch tip at position 2, 44.1 MPa.

ceased to grow. Upon closer examination, it was found that the crazes that did not grow were terminated in a pair of microshear bands [Fig. 6(a)]. These microshear bands, visible in the xy-plane when the damage zone was viewed from the side, grew into the SAN layer ahead of the craze tip. They were differentiated from the microshear bands in the PC layers that were visible in the yz-plane when the craze zone was viewed in cross section and that had initiated where the crazes impinged on the SAN–PC interface. The angle of the microshear bands in the SAN layers was 71 ± 2° compared to the 73 ± 3° angle of the microshear bands in the PC layers.

Also seen in Figure 6(b) are a few crazes that did not initiate from the notch surface but initiated some distance in front of it. These crazes generally started near the end of a terminated notch craze. It is well known that crazing can initiate from the intersection of two shear bands or at the end of a shear band,[9-11] so it is possible that these crazes initiated from the same shear bands in the SAN layers that terminated notch crazes.

Macroscopic shear yielding at the notch tip appeared in the PC/SAN 65/35 composition at about 39 MPa after the crazes had grown some distance. The two sets of intersecting slip lines growing out of the notch surface that are characteristic of the

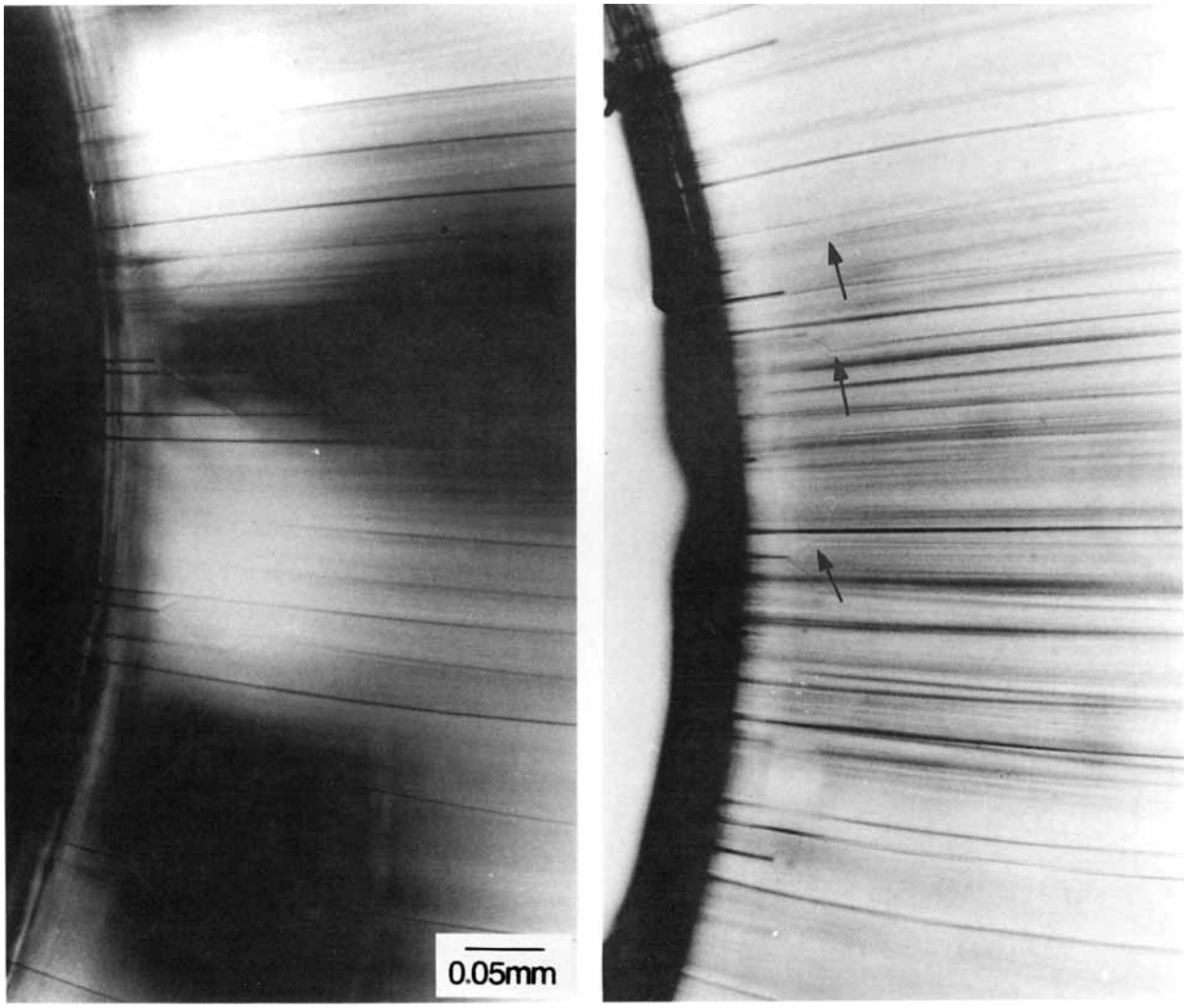

Figure 6 Higher magnification optical micrographs of the notch tip of PC/SAN 65/35 loaded to 43.7 MPa. (a) With crossed polars, and (b) the same area with a slightly different depth of focus without polars. The arrows locate crazes that initiated some distance in front of the notch tip.

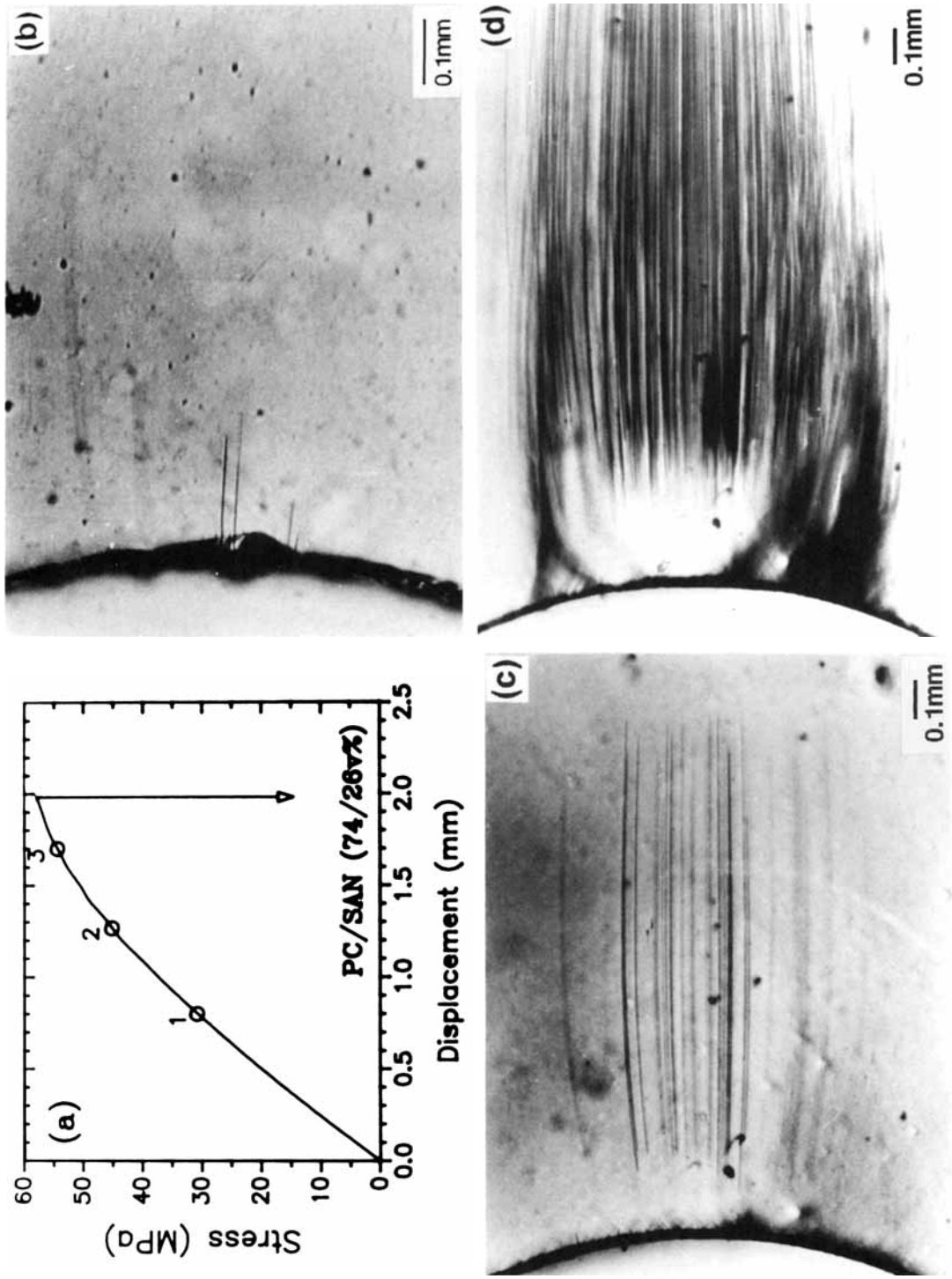

Figure 7 Tensile deformation of PC/SAN 74/26 with a semicircular notch. (a) The remote stress vs. displacement curve; (b) optical micrograph of the notch tip at position 1, 30.8 MPa; (c) optical micrograph of the notch tip at position 2, 45.1 MPa; and (d) optical micrograph of the notch tip at position 3, 54.3 MPa.

core-yielding mode in PC sheet[6] are visible in Figure 5(c). The angle of intersecting shear in the PC layers was 83 ± 1.5°. Higher stresses, about 40–45 MPa, again produced microdelamination at the crazes and macrodelamination. However, in this case macrodelamination did not occur at the notch tip, but ahead of the notch near the tip of the core-yielding zone as a consequence of stress intensification in the plastic zone. Subsequent crack propagation was slower than in the other compositions and some pullout of the PC layers created a textured fracture surface.

PC/SAN 74/26 Composition

The stress-displacement curve of this composition exhibited a longer nonlinear region than the other compositions prior to failure and had the highest failure stress and strain [Fig. 7(a)]. The first observable damage was again the internal notch crazes, although only a few were apparent in low magnification micrographs [Fig. 7(b)]. However, a view of the notch region at higher magnification revealed numerous short crazes less than 20 μm in length emanating from the notch surface, each terminating in a pair of shear bands (Fig. 8). While only a few arrested notch crazes were observed in the PC/SAN 65/35 composition, in the 74/26 composition almost all the notch crazes terminated in shear bands before they had propagated any appreciable distance from the notch surface.

The intersecting slip lines of core yielding of PC were more clearly distinguished in this composition, particularly with the focus at the center of the specimen [Fig. 7(c)]. The angle of intersection of the slip lines was 81 ± 2°. Accompanying core yielding was the appearance of a family of crazes that originated about 0.1 mm in front of the notch tip near the tip of the core-yielding zone. These crazes did not grow toward the notch, but only grew away from the notch along curved trajectories. By varying the depth of focus, it was determined that these crazes, termed internal near-notch crazes, were not surface crazes but had formed in the interior of the specimen. A few of the crazes in Figure 7(c) initiated close to the notch surface as if they had been initiated by the shear bands that terminated the short notch crazes. However, the large majority of internal near-notch crazes appeared to start about 0.1 mm from the notch near the tip of the core-yielding zone.

One half of the cross section through the internal near-notch crazes of a specimen that had been loaded to 42.1 MPa is shown in Figure 9. This section, which was made about 400 μm from the notch

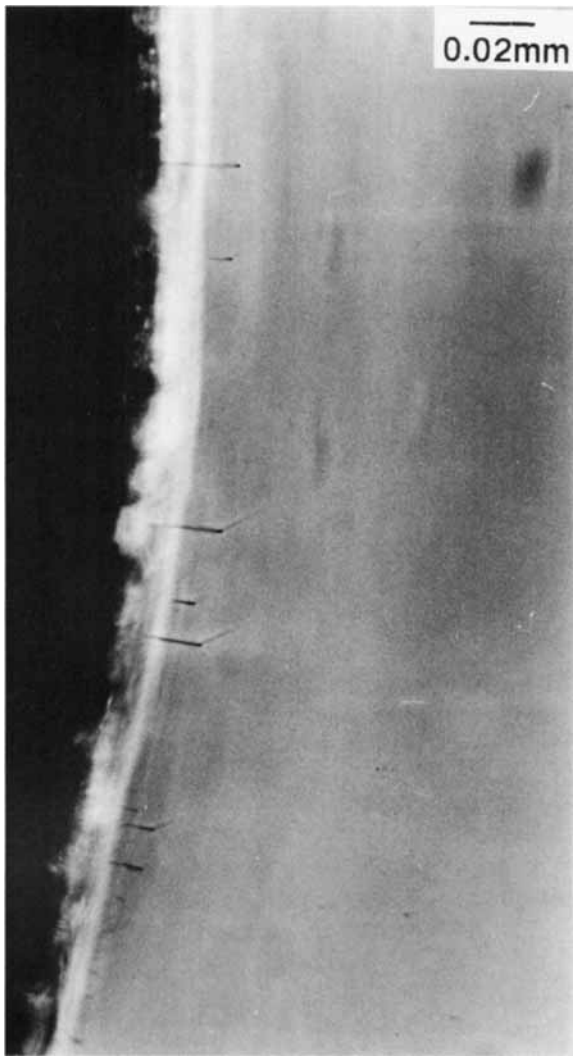

Figure 8 Higher magnification optical micrograph of the notch tip of PC/SAN 74/26 loaded to 37.1 MPa.

tip, confirmed that the near-notch crazes were located in the interior of the specimen. In this view, the near-notch crazes appeared to be very similar to the notch crazes in that they extended through the thickness of individual SAN layers; frequently a pair of shear bands formed in the adjacent PC layer where a craze impinged on the SAN–PC interface.

The more pronounced nonlinearity of the stress-displacement curve and the higher displacement at fracture were indications that shear yielding developed further in PC/SAN 74/26 than in the compositions with a lower percentage of PC. Macroscopic yielding was observed in this composition before fracture occurred. The view of the damage zone at 54.3 MPa in Figure 7(d) shows (superimposed

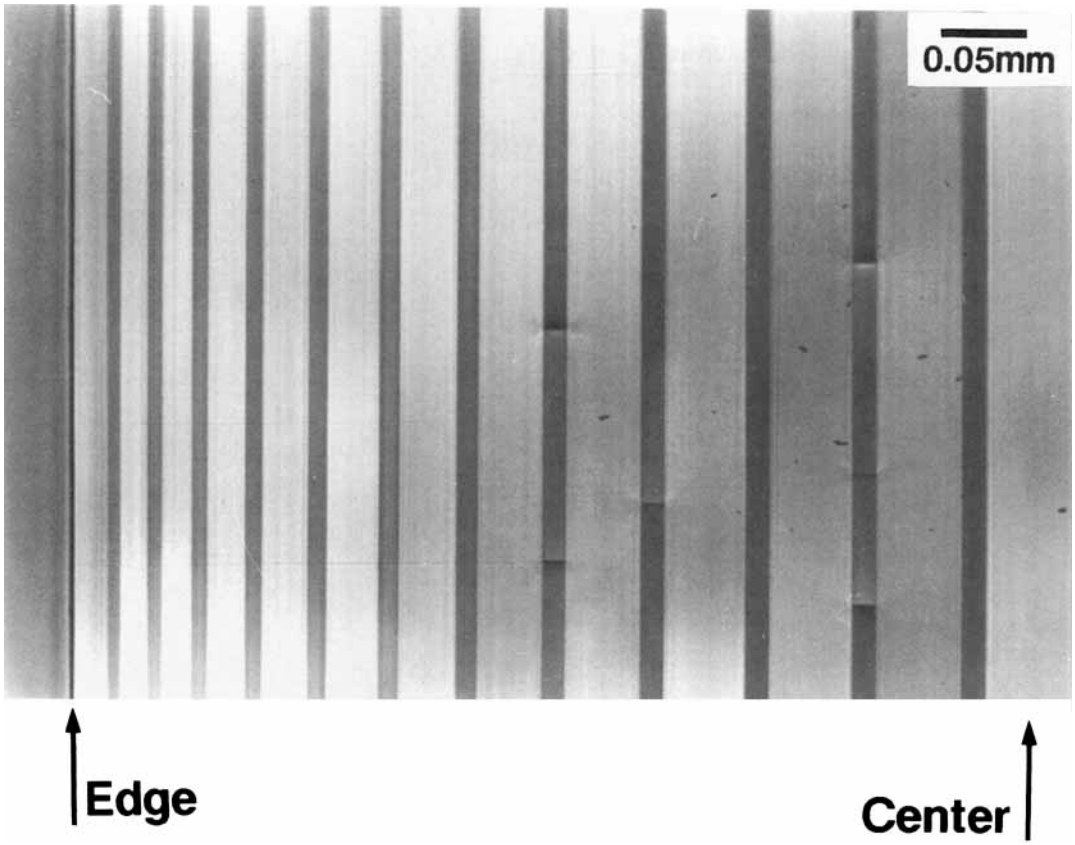

Figure 9 Microtomed cross section through the damage zone of PC/SAN 74/26 about 400 μm from the notch tip. The damage zone was created by loading the specimen to 42.1 MPa. Two arrows indicate one edge and the center of the cross section, respectively.

on the damage zone of internal near-notch crazes and a dark area of macrodelamination) a pair of wide bands that curved away from the notch above and below the x-axis. These were characteristic of the intersecting shear mode observed in thin sheet of PC.[6] This shear mode produces thinning of the cross section and global necking. Subsequent crack propagation through the highly deformed damage zone was quite fast but produced a complex fracture surface characterized by extensive delamination and drawing of the PC layers.

The cross section in Figure 10 shows the highly deformed damage zone of a specimen that had been loaded to 50.5 MPa. The section, made about 280 μm from the notch tip, illustrated the progressive stages of deformation. Beginning at the edges of the zone in the y-direction were the internal near-notch crazes through the SAN layers together with shear bands growing into the PC layers where the crazes impinged on the SAN–PC interface. As a shear band lengthened through the PC layer, it encountered another SAN layer and in certain places, for example in the lower left-hand corner of the micrograph, some of the shear bands grew through the neighboring SAN layer into the next PC layer. Closer to the midline of the zone ($y = 0$), the shear bands began to coalesce along angles of about 53° from the loading direction in the initial step toward macroscopic yielding by the intersecting shear mode. In these areas, the SAN layers fractured to accommodate the large local shear strain, and microdelamination of the SAN–PC interface at the fractured crazes was apparent. Also seen in this micrograph was the macrodelamination in the center of the specimen.

DISCUSSION

Mean-Stress Condition

The positions of the internal notch-craze tips are plotted in Figure 11 for the three compositions that exhibited this type of zone, PC/SAN 25/75, 53/47,

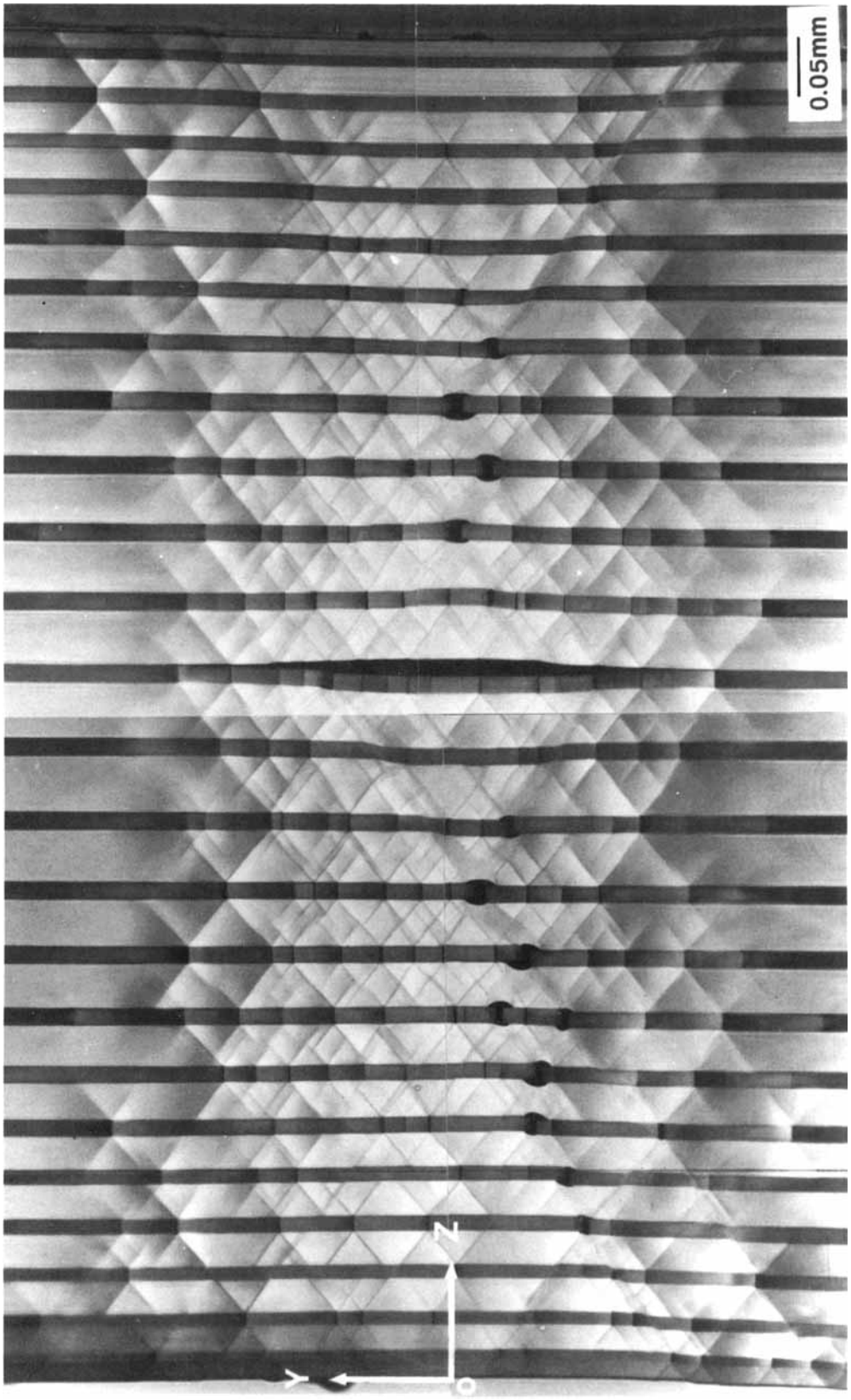

Figure 10 Microtomed cross section through the damage zone of PC/SAN 74/26 about 280 μm from the notch tip. The damage zone was created by loading the specimen to 50.5 MPa.

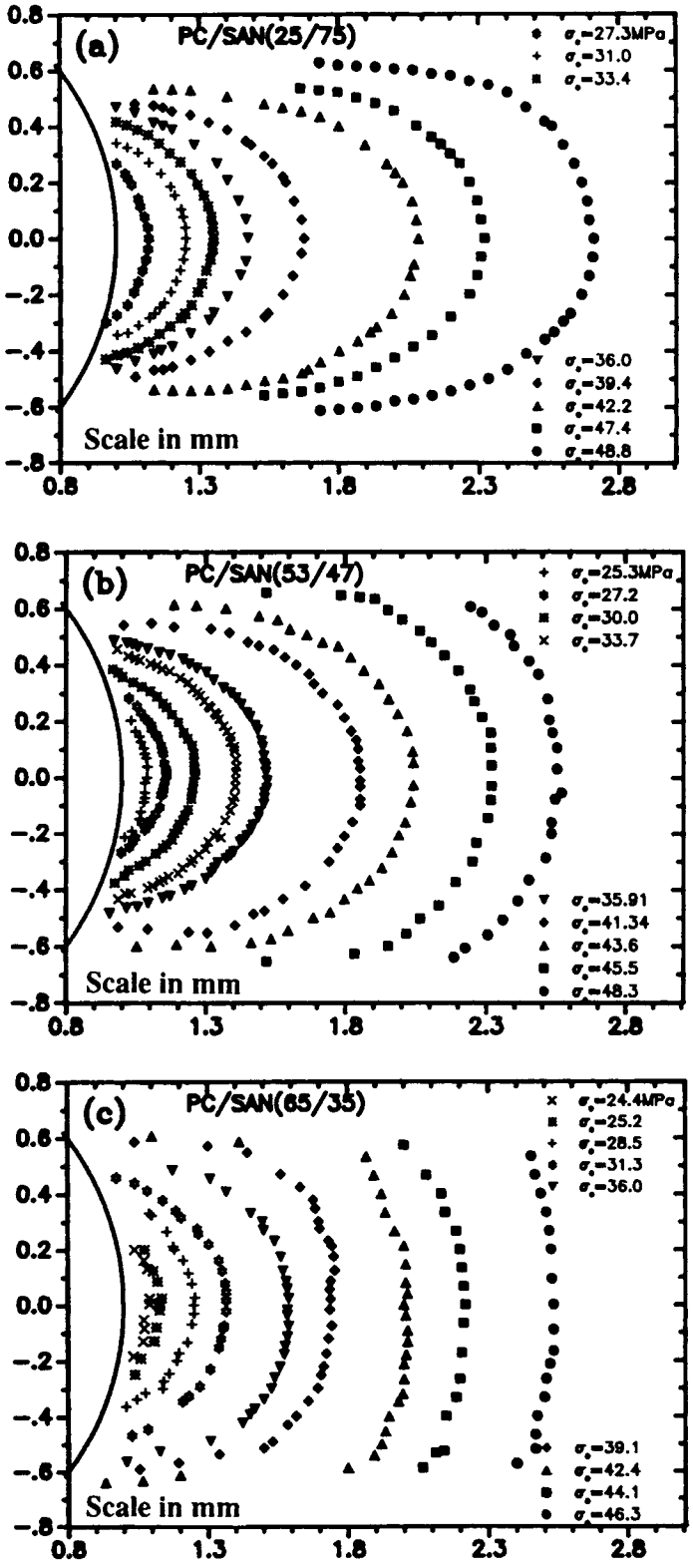

Figure 11 Positions of the internal notch-craze tips for several remote stresses. (a) PC/SAN 25/75; (b) PC/SAN 53/47; and (c) PC/SAN 65/35.

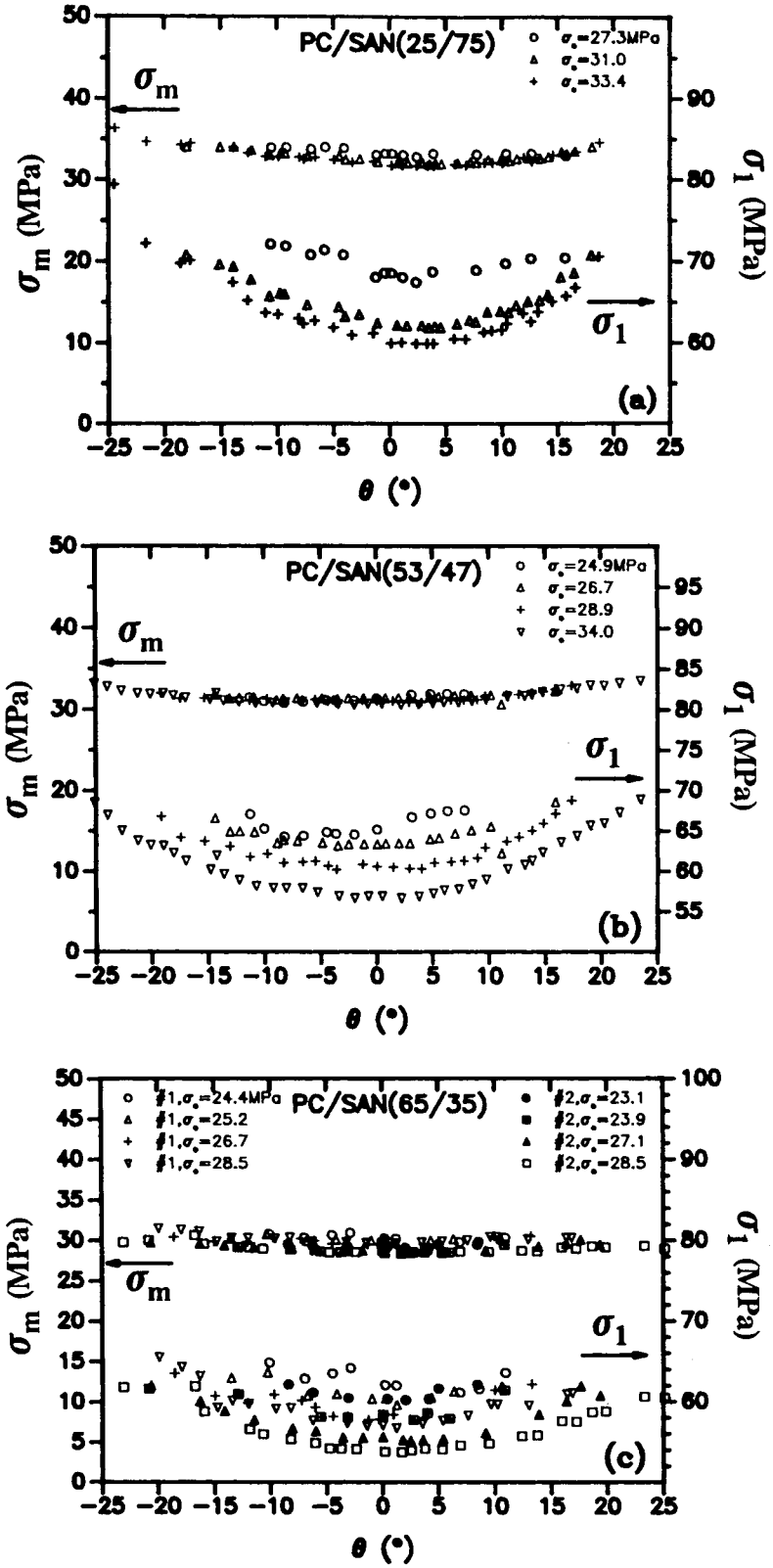

Figure 12 Mean stress (σ_m) and major principal stress (σ_1) at the positions of the craze tips for lower remote stresses as a function of the angle θ. (a) PC/SAN 25/75; (b) PC/SAN 53/47; and (c) PC/SAN 65/35.

and 65/35. The locus of these points, particularly at the lower stresses, defined a crescent shape that was analyzed according to the methodology employed previously to analyze the similar internal notch-craze zone of SAN.[7] Assuming the composite could be treated as a linear elastic solid when the zone was small, the classical elastic-stress distribution at a single semicircular notch from Maunsell's solution was used in the analysis.[12] The crescent-shaped zone defined by the craze tips resembled both σ_1 and σ_m iso-stress contours. The values of both stresses were calculated at the tip of each internal notch craze and are plotted as a function of the angle θ in Figure 12. As had been the case with SAN, the stress state at the craze tip conformed closely to a constant mean-stress condition when the zone was small, while the major principal stress exhibited a decreasing trend from the edge of the zone to the center.

Values of the critical mean stress $\sigma_{m,c}$ obtained by averaging the data in Figure 12 are listed in Table III for the three compositions. There was clearly a decrease in $\sigma_{m,c}$ as the PC content of the composite increased. The $\sigma_{m,c}$ calculation was based on the measured remote stress that was actually an average stress over a layered structure with alternating microlayers of PC and SAN in parallel. Since the two polymers had significantly different moduli and crazing occurred only in the SAN layers, the local stress in the SAN layers was calculated from the simple rule of mixtures assuming that good adhesion caused the strain to be the same in both components and any transverse shear stresses due to differences in Poisson's ratio were negligible.[13] Then, the expression for the local mean stress, $\sigma_{m\,(\mathrm{SAN})}$, is:

$$\sigma_{m\,(\mathrm{SAN})} = \frac{E_{(\mathrm{SAN})}}{E_{(\mathrm{comp})}}\,\sigma_{m\,(\mathrm{comp})} \qquad (1)$$

where E is Young's modulus. The local critical mean stress $\sigma_{m,c\,(\mathrm{SAN})}$ is also included in Table III together with the corresponding elastic-volume strain defined by $V_c = 3(1-2\nu)\,\sigma_m/E$. The local critical condition was independent of composition, and the average values of 35.5 MPa for $\sigma_{m,c\,(\mathrm{SAN})}$ and 0.96% for the corresponding local volume strain did not differ significantly from the critical conditions for internal notch crazing of SAN, 35.1 MPa and 0.95%, respectively.[7] The result that growth of internal notch crazes was controlled by the mean stress in the SAN layers even though craze growth was constrained in the thickness direction by the PC–SAN interface, confirmed previous observations that the SAN layers in the 49 layer composite were thick enough to exhibit behavior typical of SAN.[3] Subsequent interaction between crazes in SAN layers and shear bands in PC layers was the result of good adhesion between the layers so that the stress concentration created by impingement of a craze tip on the SAN–PC interface resulted in initiation of shear bands in the PC layer.

Stress Redistribution

The presence of the multiple internal notch crazes significantly affected the stress distribution around the damage zone when the damage zone became larger. One manifestation was a gradual change in shape of the zone defined by the tips of the internal notch crazes from the initial crescent shape to a shape that depended on the composition. The degree of stress redistribution was described by the concept of the mean-stress deviation $\Delta\sigma_m$, previously defined as the difference between $\sigma_{m,c}$, the mean stress that was calculated from the craze tips when the zone was small (Table III), and $\sigma_{m,E}$, the apparent elastic mean stress at the craze tip if stress redistribution were neglected, that was calculated from the elastic stress-field equation. The normalized values of $\Delta\sigma_m$ are plotted in Figure 13 as a function of θ for various remote stresses for the three compositions, 25/75, 53/47, and 65/35. It should be noted that with the

Table III Conditions for Internal Notch Craze Tip Growth in 49-Layer PC/SAN Composites

Composition (PC/SAN v %)	$\sigma_{m,c}$ (MPa)		V_c (%)	
	Average	Local (SAN)[a]	Average	Local (SAN)[a]
25/75	33.0	35.4	0.87	0.95
53/47	31.0	36.2	0.80	0.97
65/35	29.2	35.5	0.75	0.96

[a] Values calculated for SAN layer using the Rule of Mixtures.

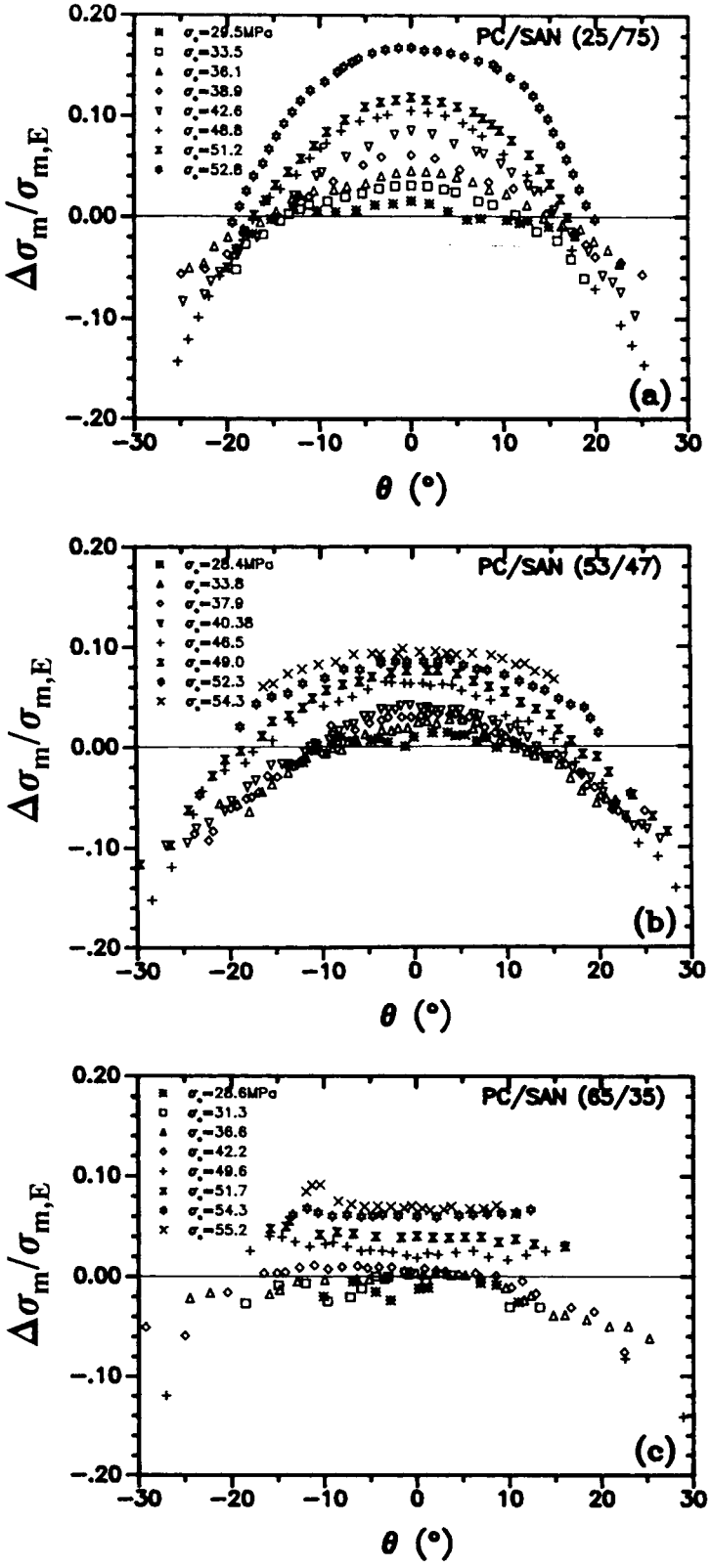

Figure 13 The normalized mean-stress deviation at the positions of the internal notch-craze tips. (a) PC/SAN 25/75; (b) PC/SAN 53/47; and (c) PC/SAN 65/35.

normalization to $\sigma_{m,E}$ it did not matter whether the average mean stress or the local mean stress in the SAN layers was used in the calculation. These plots illustrated the change in shape of the damage zone. The stress redistribution in the 25/75 composition was highest along the x-axis and decreased away from the x-axis until near the edges of the zone the crazes were shorter than anticipated from the elastic mean-stress condition. This composition most closely resembled SAN in regard to the θ dependence of the stress redistribution.[7] Stress redistribution in the 53/47 composition was also a maximum at $\theta = 0$, but was less dependent on the angle θ particularly in the center of the zone between θ angles of approximately $\pm 15°$. In the 65/35 composition the degree of stress redistribution actually increased slightly away from $\theta = 0$ to maxima at $\pm 11°$. For all compositions, $\Delta\sigma_m$ became negative, i.e., the crazes were shorter than predicted by the elastic mean-stress condition, toward the edges of the zone when the absolute value of θ exceeded $\sim 17°$.

It was also apparent that the degree of stress redistribution decreased as the composite became increasingly rich in PC. This was apparent when the degree of stress redistribution along the x-axis ($\theta = 0$) was plotted as a function of the position of the craze-zone tip for the three composites with data for SAN included for comparison[7] (Fig. 14). Constraint by the PC layers would have offset the two principal causes of stress redistribution, specifically stress intensification at the craze tip, which would have caused the craze length to exceed the length determined by the mean-stress condition, and overlapping stress fields, which would have retarded craze growth. The dependence of stress redistribution on position of the zone tip was linear for SAN and was also initially linear for the two compositions with the highest SAN content. However, the zone grew to be much longer in the composites than in SAN before fracture occurred; and as the zone lengthened, the relationship between stress redistribution and the position of the zone tip became more complex. The intermediate region of decreasing dependence on zone-tip position corresponded approximately to the region in which microdelamination at crazes was observed, and this might have served as a mechanism of localized stress or strain release. The increasing dependence prior to fracture coincided approximately with the appearance of a macrodelamination crack in the center of the specimen. Stress redistribution in the 65/35 composition was further complicated by other deformation mechanisms superimposed on the internal notch crazing, including termination of some crazes by shear bands in the SAN layer and core yielding of the PC.

Craze Trajectories

Craze trajectories of the microlayer composites were not straight but curved away from the notch as they lengthened. Careful examination of optical micro-

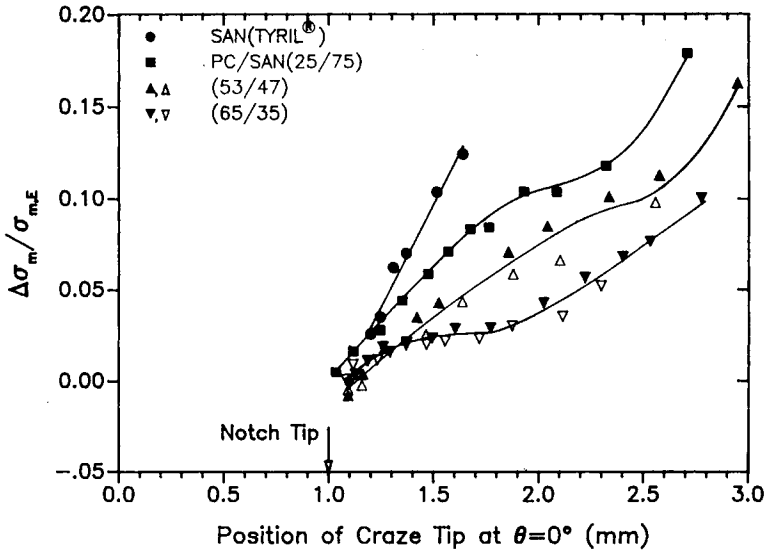

Figure 14 The normalized mean-stress deviation at the positions of the internal notch-craze tips at $\theta = 0°$. Data for SAN from ref. [7].

graphs revealed that the amount of curvature increased with increasing percentage of PC. Both straight and curved crazes were observed previously in SAN: internal notch crazes followed straight lines defined by the σ_2-vector at the point of initiation on the notch surface, while surface crazes followed closely the minor principal stress trajectory.[7] Craze trajectories in the microlayers were compared with the two limiting cases by plotting the craze slope, defined as the slope of the tangent to the craze line at any point of the craze, normalized to tan θ (Fig. 15). Only crazes that initiated at positions described by larger θ angles were analyzed since both σ_2-vectors and minor principal stress trajectories were nearly parallel to the x-axis when θ was within $\pm 10°$. While internal notch crazes in SAN had closely followed σ_2-vectors, craze trajectories in all the microlayer composites were intermediate between the σ_2-vectors and the σ_2-trajectories, with craze trajectories in the 65/35 composition somewhat closer to the σ_2-trajectories. Again, constraint by the PC layers appeared to have reduced stress redistribution in the SAN layers. The effect was more marked as the thickness of the PC layers increased relative to the SAN layers.

Plasticity

The initial irreversible deformation mechanism by which a material responds to a specific stress state is a characteristic of the material and is markedly different for the two polymers that comprised the microlayer composites. The conditions for onset of irreversible deformation under the triaxial tensile stress state at the notch tip have been described for both polymers; and while internal notch crazing of SAN responds to a cavitational or mean-stress condition, PC shear yields at the notch tip.

In analyzing the response of the microlayer composites, it was useful to compare the loading conditions required for each of these conditions to be achieved. Using the mean-stress concentration factor at a semicircular notch tip of 1.38 and the critical mean stress for cavitation of 35.1 MPa, the remote stress for craze initiation at the notch tip in SAN was calculated to be 25.4 MPa. The remote stress required for shear yielding of PC at the notch tip was 22.6 MPa, a value obtained using a tensile yield stress of 60 MPa and the von Mises yield criterion with the octahedral shear stress concentration factor at a semicircular notch of 1.258. Although shear yielding of PC was predicted to occur at a lower stress than crazing of SAN, a comparison based on remote stress was misleading because in the parallel arrangement of alternating layers the load was distributed unequally between SAN and PC layers. Assuming that distribution of the load followed the rule of mixtures, it was convenient to normalize the remote stress to the modulus to obtain a "strain" for the onset of irreversible deformation. Because of the significantly higher SAN modulus, the crazing "strain" of SAN of 0.76% was considerably lower than 0.93% for the shear yielding "strain" of PC; and it was predicted that notch crazes in the SAN layers should have preceded shear yielding of the PC layers, which would have appeared as slip lines at the notch tip.

This was illustrated with a calculation for the PC/SAN 65/35 composition using Poisson's ratio of the composite from Table I. From the plane-strain elastic analysis, the remote stress in the SAN layers would be 24.9 MPa with the mean-stress concentration factor at a notch tip of 1.41 when the mean stress in the SAN layers reached the critical value for crazing of 35.1 MPa at the notch tip. From the rule of mixtures, the average remote stress would be 20.5 MPa with the remote stress in the PC layers equal to 18.1 MPa. Under this condition, the calculated octahedral shear stress in the PC layers would be 22.9 MPa, significantly lower than the 28.4 MPa required for shear yielding.

The slip lines of core yielding were visible only in the two composites with higher percentage of PC. Consistent with the prediction, crazing in the SAN layers clearly preceded core yielding in both cases. The slip lines of core yielding were particularly evident in the 74/26 composition where the PC layers were the thickest and SAN notch crazes did not propagate to obscure the slip lines. The size and shape of the plastic zone created by core yielding and the plastic stress distribution in the zone have been described by a modified slip-line theory that takes into account the pressure-dependent yield behavior that is characteristic of most polymeric materials. In the modified theory, the slip-line field of the double logarithmic spiral is given by[14]

$$\theta \cot \psi = \pm \ln (r/a) + \text{constant} \qquad (2)$$

where 2ψ is the angle between slip lines and is related to the pressure dependency through $\mu = \cos 2\psi$; μ is defined in the modified von Mises pressure-dependent yield criterion $\kappa = \kappa_o - \mu\sigma_m$ where κ_o is the shear-yield stress at atmospheric pressure. For the 74/26 composite, the coefficient μ, calculated by the rule of mixtures from the values of the controls, 0.07

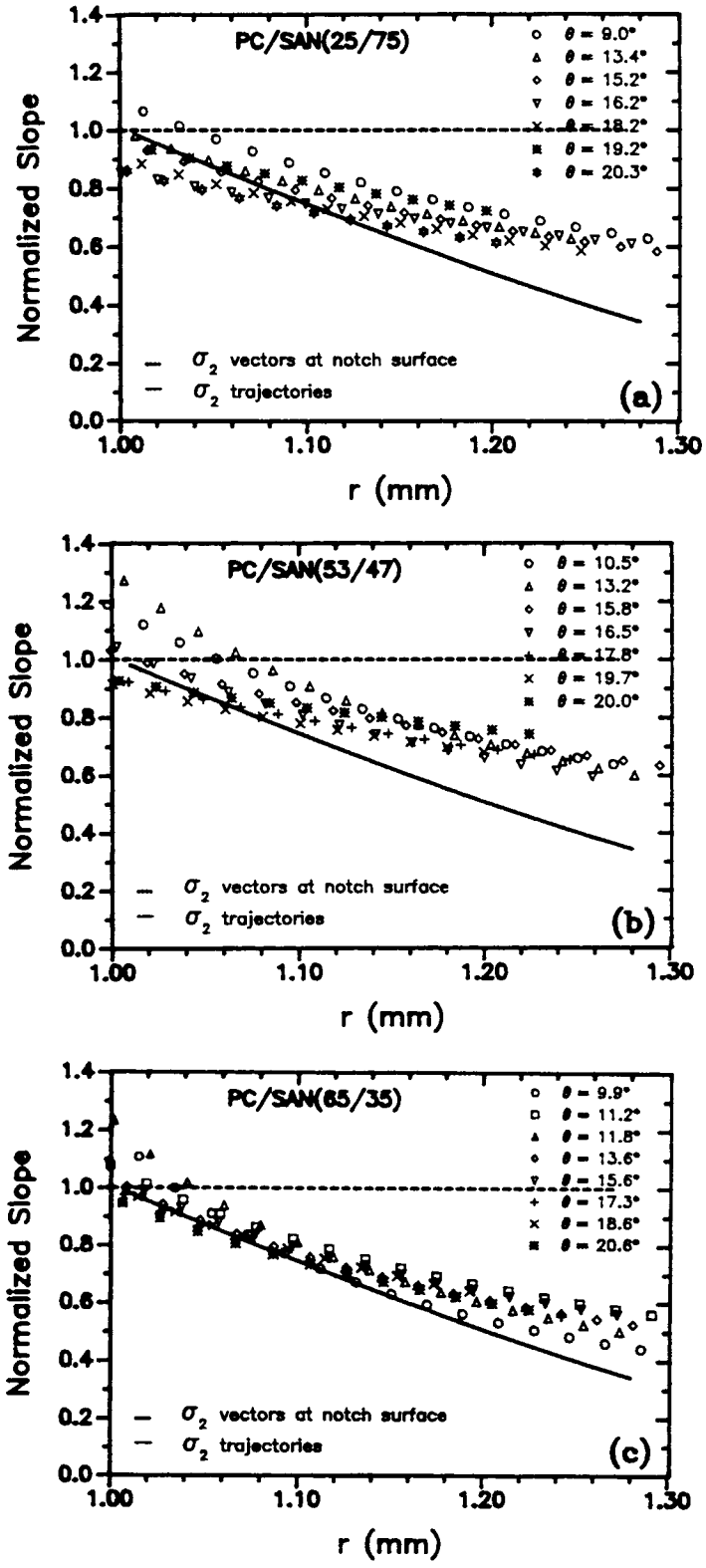

Figure 15 The slope of internal notch crazes normalized to the slope of the σ_2-vector at the position of craze initiation on the notch surface. (a) PC/SAN 25/75; (b) PC/SAN 53/47; and (c) PC/SAN 65/35.

for PC[15] and 0.178 for PS[16] assumed to be identical to SAN, was 0.10 and the corresponding angle, 2ψ, was about 80°, very close to the measured angle between slip lines, 81 ± 2°. The plastic mean stress along the x-axis in the slip-line field of a perfectly plastic material for the case of a semicircular notch is given by[14]

$$\sigma_m = \frac{\kappa_o}{\mu}\left[1 - \left(\frac{1}{1+\mu}\right)\left(\frac{r}{a}\right)^{-2\mu/(1+\mu)}\right]. \qquad (3)$$

The monotonic increase in the mean stress with the distance r from the notch tip is independent of the remote stress.

Due to the stress intensification in the plastic zone, it is not unusual to see core yielding followed by the appearance of a cavitation mechanism some distance ahead of the notch.[14,17,18] This occurred in the 74/26 composition; when shear bands prevented the internal notch crazes from lengthening, crazes initiated in the interior in response to the higher stresses in the core-yielding zone. A delamination crack subsequently formed at the same location just prior to fracture. The relationship of the plastic zone to the positions of crazing and delamination is shown in Figure 16 by overlaying an outline of the core-yielding zone calculated from eq. (2) with the damage zone. Although it was not possible to observe initiation of the near-notch crazes, it was characteristic that they propagated only away from the notch, not toward the notch. Average positions of the craze ends along the x-axis for several remote stresses are plotted in Figure 17. Intersection of the curve that described the craze boundary further from the notch with the position of the boundary near the notch suggested that near-notch crazes initiated at a remote stress of approximately 35 MPa.

It was assumed that core yielding occurred in the SAN layers as well as the PC layers since no delamination was observed in the core-yielding zone. The local mean stress in the plastic zone was then calculated from eq. (3), and a value of 37 MPa was obtained at the position 0.1 mm from the notch tip using a value of 36.0 MPa for κ_o the shear-yield stress of the composite.[2] However, eq. (3) describes a homogeneous plastic zone, and caution had to be used in assigning quantitative significance to the value of 37 MPa, even though it was numerically similar to the mean-stress condition for craze-tip growth of 35.1 MPa obtained in the elastic analysis of the internal notch-craze zone of SAN and the brittle microlayer compositions. The position of the near-notch craze tips could have represented a craze-tip growth condition or alternatively a craze-initiation condition. One possible interpretation was that crazes initiated when the tip of the plastic zone reached a distance 0.1 mm from the notch tip. Since this was the elastic–plastic boundary when craze initiation occurred, the rule of mixtures calculation gave a mean stress in the SAN layers of 46.7 MPa. The difference between this value and 35.1 MPa reflected the difference between the conditions for craze initiation and craze growth. On the other hand, craze initiation might have occurred further from

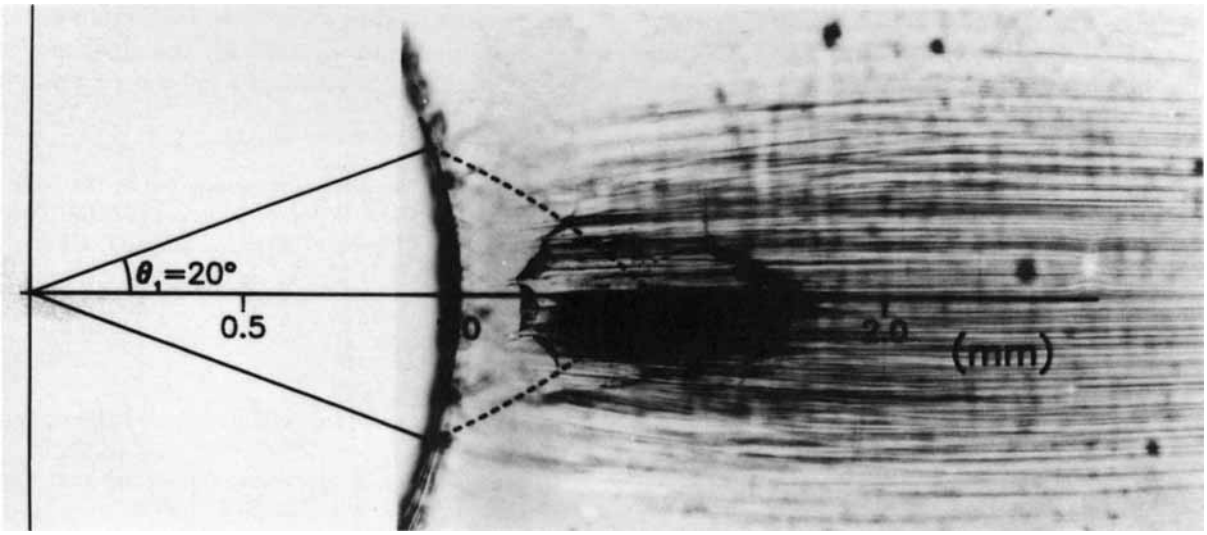

Figure 16 The damage zone of PC/SAN 74/26 at 50.5 MPa overlayed with the outline of the core-yielding zone.

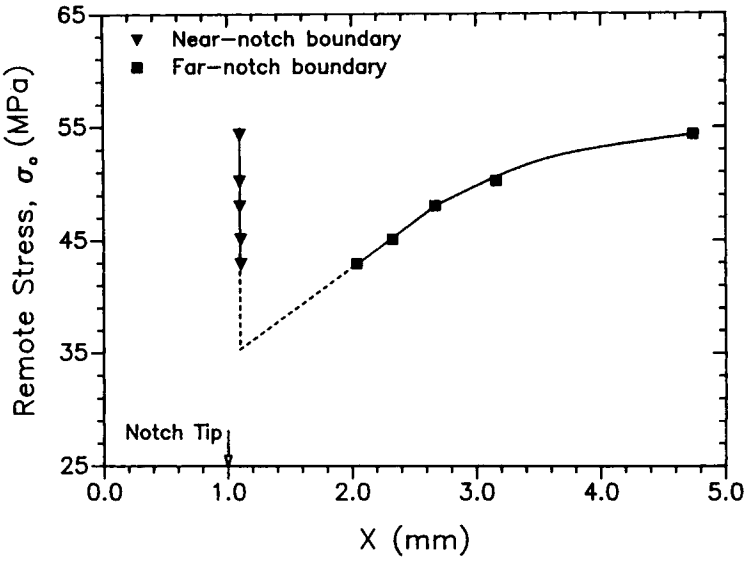

Figure 17 Positions of the near-notch craze ends of PC/SAN 74/26 at several remote stresses.

the notch and the position 0.1 mm from the notch represented the condition for craze growth in the yielded zone. In this case the rule of mixtures would not apply and it was not possible to estimate the local mean stress in the SAN layers. In support of the latter interpretation, growth of polystyrene crazes in shear-yielded material is well documented and thought to occur quite easily.[19,20]

CONCLUSIONS

The irreversible deformation behavior of coextruded microlayer composites that consisted of 49 alternating layers of PC and SAN was examined in a triaxial stress state. Analysis of the damage zone that formed at a semicircular notch during slow tensile loading led to the following conclusions:

1. The initial irreversible deformation consisted of continuous internal notch crazes in the SAN layers. In the three compositions with the highest proportion of SAN, the damage zone defined by the internal notch crazes closely resembled that of SAN even though the crazes were unable to grow in the thickness direction where they were constrained by the SAN–PC interface. Shear bands initiated in the PC layers where crazes impinged on the SAN–PC interface.
2. Shear processes became more evident as the proportion of PC increased. In the region of the notch tip, internal notch crazes ceased to grow when they terminated in a pair of microshear bands in the SAN layer. A macroscopic shear-yielding mode was also observed. The two sets of intersecting slip lines that are characteristic of core yielding in PC were observed growing out of the notch surface.
3. Stress intensification caused by the presence of a plastic zone at the notch tip was responsible for the appearance of near-notch crazes. This second family of internal crazes originated a short distance in front of the notch tip and grew away from the notch. Delamination midway through the thickness also occurred near the tip of the core-yielding zone.

This research was generously supported by the National Science Foundation, Polymers Program (DMR 9100300), and The Dow Chemical Company, Midland, MI.

REFERENCES

1. B. L. Gregory, J. Im, A. Hiltner, and E. Baer, *Polym. Eng. Sci.*, **27**, 568 (1987).
2. B. L. Gregory, A. Siegmann, J. Im, A. Hiltner, and E. Baer, *J. Mater. Sci.*, **22**, 532 (1987).
3. M. Ma, K. Vijayan, J. Im, A. Hiltner, and E. Baer, *J. Mater. Sci.*, **25**, 2039 (1990).
4. M. Ma, J. Im, A. Hiltner, and E. Baer, *J. Appl. Polym. Sci.*, **40**, 669 (1990).

5. J. Im, A. Hiltner, and E. Baer, in *High Performance Polymers;* E. Baer and A. Moet, Eds., Hanser, New York, 1991, p. 175.
6. M. Ma, K. Vijayan, A. Hiltner, and E. Baer, *J. Mater. Sci.,* **24,** 2687 (1989).
7. E. Shin, A. Hiltner, and E. Baer, *J. Appl. Polym. Sci.,* **46,** 213–230 (1992).
8. J. Keitz, J. Barlow, and D. Paul, *J. Appl. Polym. Sci.,* **29,** 3131 (1984).
9. N. J. Mills, *J. Mater. Sci.,* **11,** 363 (1976).
10. M. Ishikawa, I. Narisawa, and H. Ogawa, *J. Polym. Sci. Polym. Phys. Ed.,* **15,** 1791 (1977).
11. M. Ishikawa and I. Chiba, *Polymer,* **31,** 1232 (1990).
12. F. G. Maunsell, *Phil. Mag.,* **21,** 765 (1936).
13. C. X. Zhu, S. Umemoto, N. Okui, and T. Sakai, *J. Mater. Sci.,* **23,** 4091 (1988).
14. M. Kitagawa, *J. Mater. Sci.,* **17,** 2514 (1982).
15. A. W. Christiansen, E. Baer, and S. V. Radcliffe, *Phil. Mag.,* **24,** 451 (1971).
16. K. Matsushige, S. V. Radcliffe, and E. Baer, *J. Mater. Sci.,* **10,** 823 (1975).
17. I. Narisawa, M. Ishikawa, and H. Ogawa, *J. Mater. Sci.,* **15,** 2059 (1980).
18. A. Tse, E. Shin, A. Hiltner, and E. Baer, *J. Mater. Sci.,* **26,** 5374 (1991).
19. C. C. Chau and J. C. M. Li, *J. Mater. Sci.,* **16,** 1858 (1981).
20. J. C. M. Li, *Polym. Eng. Sci.,* **24,** 750 (1984).

Received January 27, 1992
Accepted March 2, 1992